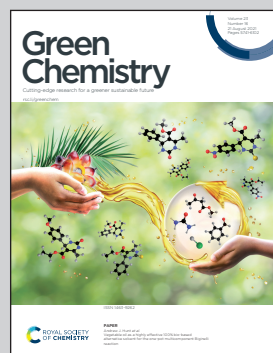


An article presented by Associate Professor Masazumi Tamura from Osaka City University, Japan and Professor Keiichi Tomishige from Tohoku University, Japan.

Direct synthesis of polycarbonate diols from atmospheric flow CO₂ and diols without using dehydrating agents

Polycarbonate diols were directly synthesized from diols and CO₂ over a heterogeneous CeO₂ catalyst, and high yields (up to 92%) of target polycarbonate diols were obtained. CeO₂ exhibited its unique catalytic activity towards the reaction under atmospheric pressure, and the efficient removal of the coproduced water by gas stripping with the CO₂ flow reaction system was vital to overcoming the thermodynamic limitation. The process can be an environmentally friendly alternative to the conventional processes using toxic phosgene and CO as raw materials.

As featured in:



See Masazumi Tamura,
Keiichi Tomishige *et al.*,
Green Chem., 2021, **23**, 5786.



Cite this: *Green Chem.*, 2021, **23**, 5786

Direct synthesis of polycarbonate diols from atmospheric flow CO_2 and diols without using dehydrating agents†

Yu Gu, ^a Masazumi Tamura, *^b Yoshinao Nakagawa, ^a Kenji Nakao, ^c Kimihito Suzuki and Keiichi Tomishige *^a

Polymer synthesis with CO_2 as a C1 chemical has attracted much attention from the viewpoint of green chemistry. The direct transformation of CO_2 and diols into polycarbonate diols is promising as an alternative method to the hazardous phosgene process, however, challenging due to the inert characteristic of CO_2 and thermodynamic limitation. Herein, we present the direct synthesis of polycarbonate diols from atmospheric pressure CO_2 and α,ω -diols using a heterogeneous CeO_2 catalyst and a CO_2 flow semi-batch reactor. The target alternating polycarbonate diol from CO_2 and 1,6-hexanediol was obtained with high yield (92%) and selectivity (97%) without using any dehydrating agents. Activation of atmospheric pressure CO_2 by a CeO_2 catalyst and the shift of equilibrium towards the product by removing the coproduced water (gas stripping) are responsible for the high yield. The flow reaction system with a CeO_2 catalyst was applicable to the reactions of CO_2 and primary mono-alcohols or 1,2-diols, giving the target organic carbonates in high selectivity (>99%).

Received 6th April 2021,
Accepted 29th June 2021
DOI: 10.1039/d1gc01172c
rsc.li/greenchem

Introduction

The reduction of CO_2 in the atmosphere is an urgent issue for mankind to achieve a sustainable society because of global warming and related problems such as abnormal weather, sea level rise, ecological system change, and so on. CO_2 is renewable, abundant, cheap, non-flammable and non-toxic, and the transformation of CO_2 as a C1 source into valuable chemicals is one of the promising strategies.^{1–5} Various effective catalyst systems have been developed for the reductive transformation of CO_2 into methanol, CO, hydrocarbons, formic acid, etc.^{6–20} and for the non-reductive transformation into organic carbonates, carbamates, ureas, and their polymers.^{20–47} Organic carbonates such as dialkyl carbonates, cyclic carbonates, and polycarbonates are valuable chemicals and conventionally made by the phosgene process with problems such as the use of hazardous phosgene and dichloromethane, and the pro-

duction of waste salt from the reaction with sodium hydroxide.^{28–31} The direct conversion of CO_2 with alcohols to the carbonates can be an ideal substitute because water is the only by-product, and the substrates are easily available and safe. However, the high yield synthesis of organic carbonates, especially polycarbonates, is difficult because of the low reactivity of CO_2 and low yield restricted by the equilibrium (Fig. 1).^{28–31,48} CeO_2 -based catalysts have been reported to be effective heterogeneous ones for the reaction owing to the high potential for CO_2 activation and the equilibrium yields of the corresponding dialkyl carbonates were lower than 2% even with pressurized CO_2 up to 20 MPa.^{28–31} It is reported that high CO_2 pressure is required for the spontaneous progress of the reaction (e.g., $\Delta G < 0$, $P_{\text{CO}_2} > 2.41 \times 10^4$ MPa in the dimethyl carbonate synthesis at 353 K, theoretically).⁴⁹ Such enormous pressure is technically difficult and consequently, the coproduced water should be removed to shift the equilibrium to the product side. Various dehydration systems equipped with membranes,^{50,51} physical adsorbents,^{41,52–55} and chemical dehydrating agents^{56–68} have been developed (Fig. 1). Membranes such as inorganic ceramic membranes and organic polymer membranes^{50,51} and physical adsorbents such as molecular sieves^{52–55} provided low yields of organic carbonates despite the high CO_2 pressure (0.4–30 MPa), and the low durability, regeneration treatment, and/or complex reaction system are also problematic. The synthesis combined with a reactive dehydration reaction using chemical dehydrat-

^aDepartment of Applied Chemistry, School of Engineering, Tohoku University, 6-6-07 Aoba, Aramaki, Aoba-ku, Sendai, 980-8579, Japan.

E-mail: tomi@erec.che.tohoku.ac.jp

^bResearch Center for Artificial Photosynthesis, The Advanced Research Institute for Natural Science and Technology, Osaka City University, 3-3-138 Sugimoto, Sumiyoshi, Osaka, 558-8585, Japan. E-mail: mtamura@osaka-cu.ac.jp

^cNippon Steel Corporation, 20-1 Shintomi, Futsu, Chiba, 293-8511, Japan

† Electronic supplementary information (ESI) available. See DOI: 10.1039/d1gc01172c



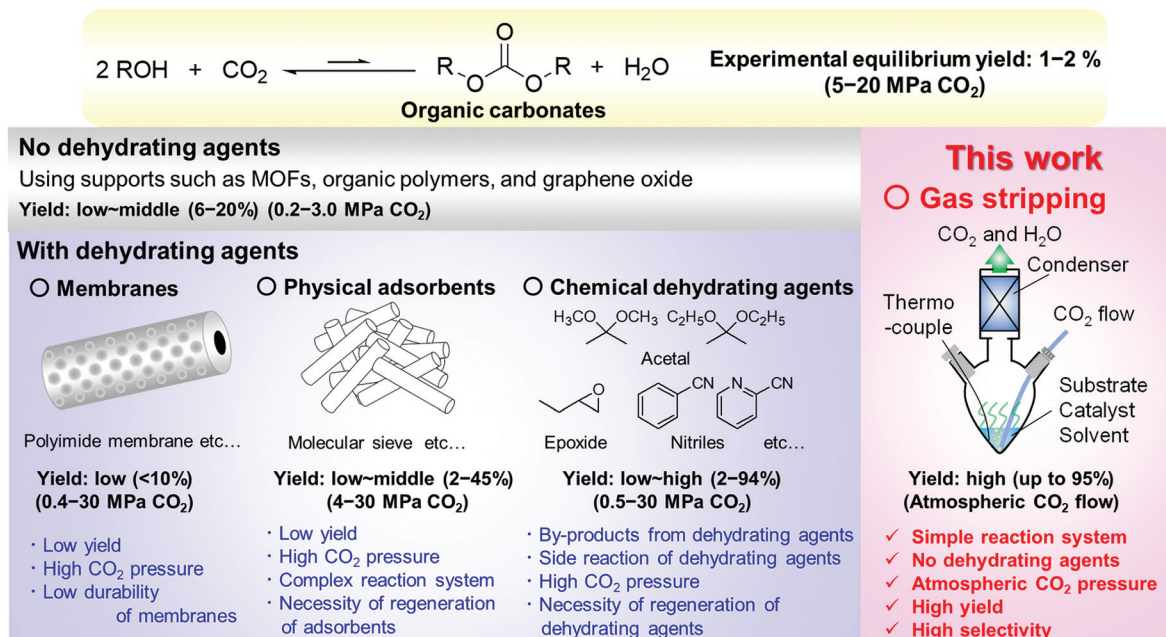


Fig. 1 Direct synthesis of organic carbonates from CO_2 and alcohols with/without dehydration systems and the strategy of this work.

ing agents such as nitriles, acetals, epoxides, ionic liquids, and so on has been regarded as effective systems.^{56–69} A handful of dehydrating agents including 2-cyanopyridine,^{62–64} cyanopyrazine,^{62,64} and 2-furonitrile⁶⁰ with a CeO_2 catalyst enabled sufficient removal of water to shift the equilibrium to the product side and provided over 90% yield of dialkyl carbonates. Various problems for industrialization, however, remain unsolved, including the regeneration of the dehydrating agents, high CO_2 pressure, formation of dehydrating agent-derived by-products, and decomposition of dehydrating agents.^{56,59,60,64} On the other hand, the synthesis of dialkyl carbonates from CO_2 and alcohols without using dehydrating agents has also been reported. Ti-Based and Cu–Ni-based MOFs and graphene oxide immobilized $\text{Cs}_2\text{Mo}_6\text{Br}_{14}$ provided 6–20% yield of the dialkyl carbonates,^{70–73} and the catalysts themselves may play a role in H_2O removal from the reaction system.^{31,72}

Polymers are essential materials in our life, and the development of greener synthesis methods for them is indispensable to attain a sustainable society. In this context, the direct synthesis of polymers from CO_2 is a hot topic, and various effective reaction systems with suitable chemicals and/or catalysts have been developed: CO_2 can polymerize with cyclic ethers (epoxides and oxetanes) to polycarbonates,^{21–25,40} alkenes or alkynes to polyesters,^{74–76} dihalide and diols to polycarbonates,^{77,78} diols to polycarbonates,^{59,60,79,80} and diamines to polyureas,^{81–83} and so on.⁸⁴ Polycarbonates are useful chemicals with high demand (4.3 million tons in 2015, and expected to reach 7.7 million tons by 2024⁸⁵) as engineering plastics and intermediates for the production of polyurethanes. Polycarbonates have been conventionally produced by using phosgene, which has many drawbacks such as the high toxicity of phosgene, use of a large amount of

solvents and caustic sodium hydroxide, and formation of a large amount of waste salt by neutralization.^{25,59,85} As an alternative method, the Asahi Kasei process was industrialized in 2012 using CO_2 as the carbonyl source, and the process is composed of four steps including the carbonate synthesis from ethylene oxide and CO_2 , and transesterification of carbonates and alcohols.^{86,87} Considering the versatility, availability and handling ability of alcohols, the direct synthesis of polycarbonates from CO_2 and diols is a promising process. The atom efficiency of the reaction is higher than those of the reactions applied in other processes (direct process: 94%, phosgene process: 63%, Asahi Kasei transesterification process: 81% in the case of bis(6-hydroxyhexyl)carbonate synthesis from CO_2 and 1,6-hexanediol. Formulas are shown in Fig. S1†). Despite the theoretical advantages, the reaction of CO_2 and diols has only been reported with additional reagents: alkyl α,ω -dihalides were used as a co-reactant with CO_2 and diols under 1 MPa CO_2 , affording polycarbonates with an M_n of 22 000 g mol^{−1}.⁷⁷ A CeO_2 catalyst with nitrile dehydrating agents such as 2-cyanopyridine and 2-furonitrile was also reported to be effective for the polymerization of CO_2 and α,ω -diols under 5 MPa CO_2 , producing the polycarbonates with M_n values lower than 6000 g mol^{−1} due to the nitrile-related side reactions (a detailed comparison of these works is shown in Table S1†).^{59,60,79,80} The high pressure of CO_2 and use of dihalides and nitriles are not preferable and the development of a practical and hazardous reagent-free process for the synthesis of polycarbonate diols from low-pressure CO_2 and diols is highly required.

Gas stripping is a separation process, wherein a gas passes through a liquid mixture to selectively remove some components with lower boiling points from the liquid phase.^{88,89} As for the synthesis of polycarbonate diols from CO_2 and diols,



the boiling points of diols and the target polycarbonate diols can be adequately higher than that of H_2O , and flowing CO_2 will serve as a reactant as well as a stripper for the removal of the coproduced water. Therefore, we envisioned that a high yield of target polycarbonate diols can be obtained by selectively removing the coproduced water from the reaction media by gas stripping with CO_2 flow and shifting the equilibrium to the product side if diols can react with atmospheric pressure CO_2 by using an appropriate catalyst. It is necessary to precisely control the reaction conditions such as reaction temperature, solvents, CO_2 flow rate, and so on to decrease the water concentration of the reaction media to a low level.

Herein, we found that the combination of a CeO₂ catalyst and CO₂ flow reaction setup with gas stripping was an effective reaction system for the direct synthesis of polycarbonate diols from atmospheric CO₂ and diols.

Results and discussion

Application of a CO_2 flow semi-batch reactor in the reaction of 1,6-hexanediol and CO_2 over CeO_2

We commenced with the reaction of 1,6-hexanediol and flow CO_2 at atmospheric pressure over CeO_2 , which is a well-known catalyst for this type of reaction as mentioned above, in triethylene glycol dimethyl ether (triglyme) solvent at 473 K by using a CO_2 flow semi-batch reactor (Fig. 2a, the details of the reactor are shown in Fig. S2†). The boiling points of 1,6-hexanediol (522 K) and triglyme solvent (489 K) are higher than the reaction temperature of 473 K, however, their vaporization under the gas flow conditions leads to material loss. A condenser was connected to the outlet of the flask and the temperature was set to 297 K to trap the vaporized substrate and solvent in the gas flow. Triglyme was selected as a solvent because it can dissolve 1,6-hexanediol, and the solidified 1,6-hexanediol (melting point: 315 K) at the condenser was rinsed away with the trapped triglyme. The reaction of flow CO_2 and 1,6-hexanediol proceeded smoothly to reach 50% yield in 24 h with a high diol balance (>99%) (Fig. 2a). The corresponding dimer, bis(6-hydroxyhexyl) carbonate, was formed as the sole product until 4 h, and the formation of the polymer, which is defined as a trimer and further polymerized products in this paper, appeared at a longer reaction time. The water content in the reaction media measured by coulometric Karl-Fischer titration (Fig. S3†) was below the detection limit (<4 ppm), suggesting that the coproduced water was efficiently removed from the reaction media. The amount of the coproduced water at the initial 4 h is calculated to be 1.0 mmol (0.018 g) from the conversion. Assuming that all the coproduced water was diffused to the gas phase at a constant rate, the water concentration at a gas flow rate of 200 mL min^{-1} can be estimated to be 0.38 g m^{-3} , which is far below the water concentration of saturated water vapor at 297 K (condenser temperature), 22 g m^{-3} . Therefore, the coproduced water in the gas flow cannot be trapped in the condenser.

To check the equilibrium level in a sealed batch reactor under atmospheric pressure CO_2 , 1,6-hexanediol was reacted

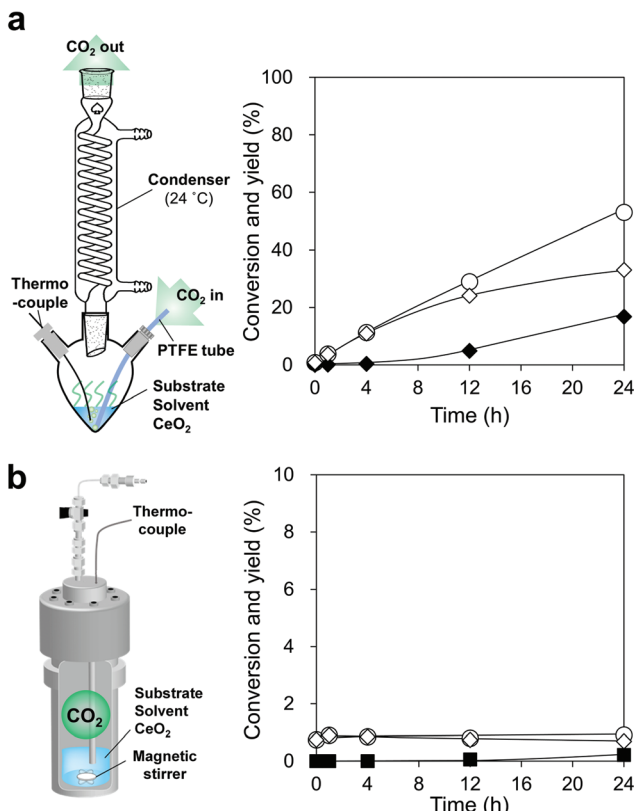
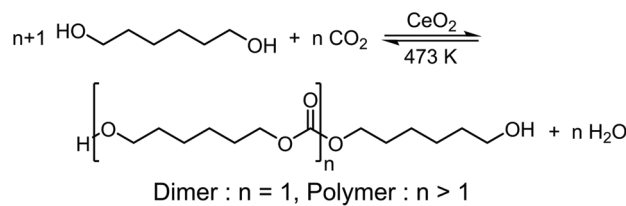


Fig. 2 Reaction of CO_2 and 1,6-hexanediol over CeO_2 with two different reactors: (a) CO_2 flow semi-batch reactor and time-course under atmospheric CO_2 flow and (b) sealed batch reactor and time-course under 7.5 MPa CO_2 . O, Conversion; \diamond , dimer yield; \blacklozenge , polymer yield; and \blacksquare , Others yield (Others include ester and ether). Reaction conditions: (a) CeO_2 0.10 g, 1,6-hexanediol 2.0 g (17 mmol), triglyme 3 g, 473 K, CO_2 flow rate 200 mL min^{-1} . (b) CeO_2 0.10 g, 1,6-hexanediol 2.0 g (17 mmol), triglyme 3 g, 473 K, CO_2 7.5 MPa, the detailed data are shown in Table S2.[†]

with 0.1 MPa of CO₂ in an autoclave reactor, giving the result that the formation amount of the target carbonate was below the detection limit (yield < 0.01%, Table S3†). Even in the reaction with high-pressure CO₂ (7.5 MPa) in the sealed batch reactor (Fig. 2b), the conversion was low and became constant at 0.9% (4–24 h) with a dimer produced as the main product. These results indicate that the equilibrium yield at high CO₂ pressure (7.5 MPa) is about 1%, and the equilibrium yield with atmospheric pressure CO₂ at 473 K in the sealed batch reactor can be estimated to be below 0.01%. The water content of the reaction mixture in the sealed batch reactor under 7.5 MPa was 600–700 ppm (Fig. S3†), which was mainly from the water impurity of the reagents and the coproduced H₂O from the carbonate formation. The water amount was clearly higher than

that in the CO_2 flow semi-batch reactor. As a result, the conversion in the CO_2 flow semi-batch reactor largely exceeded the equilibrium level, which is hardly achievable in a sealed-batch reactor without dehydrating agents. As above, the coproduced water in the CO_2 flow semi-batch reactor can be removed from the reaction media, leading to high conversion and yields by shifting the chemical equilibrium to the product side.

Effect of reaction parameters on the reaction of 1,6-hexanediol and CO_2 in a CO_2 flow semi-batch reactor

To confirm the specificity of CeO_2 for the reaction in a CO_2 flow semi-batch reactor, the reactions without a catalyst and with various solid oxides were carried out (Table S4†). No products were detected without using a catalyst (yield < 0.01%). CeO_2 exhibited excellent catalytic activity towards the reaction of flow CO_2 and 1,6-hexanediol under atmospheric pressure, giving 17% conversion of the diol and >99% selectivity to organic carbonate species including the dimer and the polymer. In the cases of $\gamma\text{-Al}_2\text{O}_3$ and $\text{SiO}_2\text{-Al}_2\text{O}_3$, there were no carbonate products, while linear and cyclic ethers of 1,6-hexanediol were produced as major products with 5-hexen-1-ol and its isomers as minor products. The strong acidity of these catalysts is reported to be responsible for their catalytic activity.^{90–92} Other metal oxides used in the experiments were inactive, and no products were obtained. The initial formation rate of the dimer with

CeO_2 was found to be $15 \text{ mmol g}_{\text{cat}}^{-1} \text{ h}^{-1}$ (Fig. S4†), which is adequately high compared with the previous reports ($0.1\text{--}11 \text{ mmol g}_{\text{cat}}^{-1} \text{ h}^{-1}$) using organic dehydrating agents except for the cases with 2-cyanopyridine ($75 \text{ mmol g}_{\text{cat}}^{-1} \text{ h}^{-1}$),²⁸ CCl_3COOMe ($70 \text{ mmol g}_{\text{cat}}^{-1} \text{ h}^{-1}$),²⁸ and 2,2-diethoxypropane ($44 \text{ mmol g}_{\text{cat}}^{-1} \text{ h}^{-1}$).⁶¹ Therefore, the catalyst system is quite meaningful from the practical viewpoint.

Various reaction parameters were investigated in the same reaction (Fig. 3). The conversion at 1 h was plotted as a function of the CeO_2 amount (Fig. 3a), showing that the conversion increased with the increase of the CeO_2 amount in the range of 0–0.08 g and reached 3.8% in this range. The reaction progress was controlled by the catalyst amount in the range of 0–0.08 g, indicating that the rate-determining factor is the catalytic activity of CeO_2 in the reaction of 1,6-hexanediol with CO_2 . With larger amounts of CeO_2 from 0.08 to 0.20 g, the conversion became constant at 3.8%, indicating that the rate-determining factor here is the removal of water from the reaction media.

Next, the solvent effect on the reaction was investigated with an adequate amount of the CeO_2 catalyst (0.10 g). The reaction under the neat conditions provided a similar conversion to the previous case, however, the diol balance decreased to 87%, and the solidified 1,6-hexanediol was observed in the condenser (Fig. S5 and S6†), leading to a block of the flow line at a longer reaction time. Other solvents with high boiling

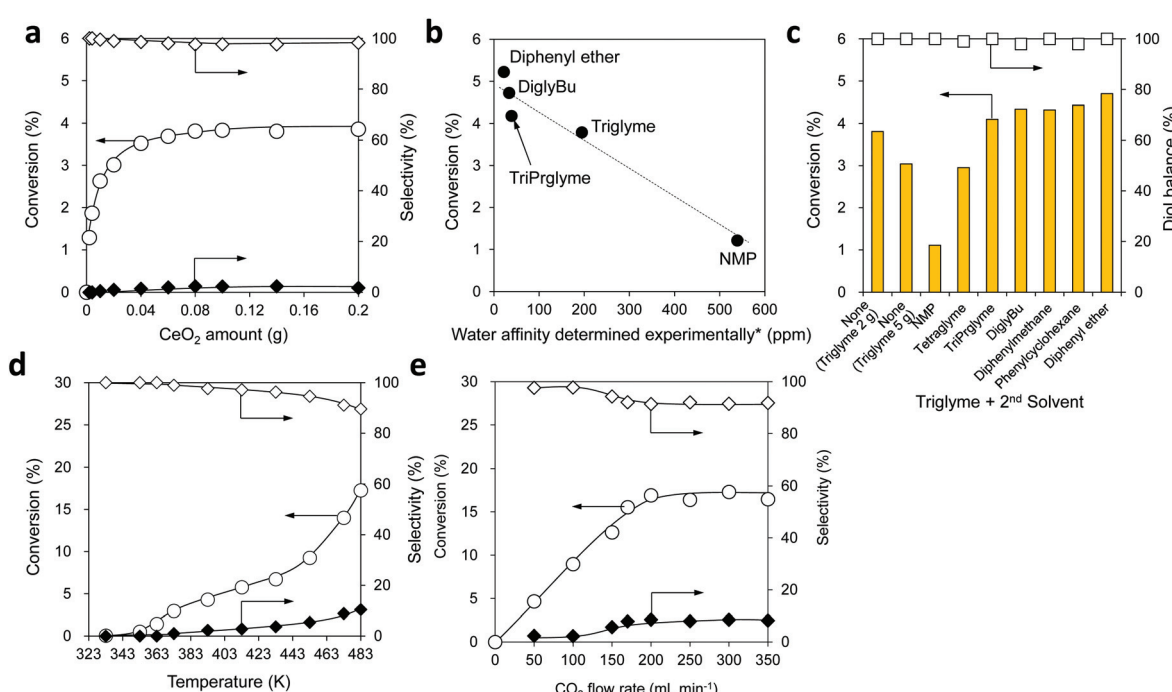


Fig. 3 Effect of reaction parameters: (a) CeO_2 amount, (b) relationship between the water affinity of solvents and the conversion, (c) solvent effect, (d) reaction temperature, and (e) CO_2 flow rate. Marks in (a), (d) and (e): \circ , Conversion; \diamond , dimer selectivity; and \blacklozenge , polymer selectivity. Mark and bar in (c): \square , Diol balance; bar, conversion. *The ability of solvents to retain water under the reaction conditions. Reaction conditions: (a) CeO_2 0–0.20 g, 1,6-hexanediol 2.0 g (17 mmol), triglyme 3 g, CO_2 flow rate 200 mL min^{-1} , 473 K, 1 h. (b) CeO_2 0.10 g, 1,6-hexanediol 2.0 g (17 mmol), solvent 3 g, CO_2 flow rate 200 mL min^{-1} , 473 K, 1 h. (c) CeO_2 0.10 g, 1,6-hexanediol 2.0 g (17 mmol), triglyme 2 g, 2nd solvent 0 or 3 g, CO_2 flow rate 200 mL min^{-1} , 473 K, 1 h. (d) CeO_2 0.10 g, 1,6-hexanediol 2.0 g (17 mmol), triglyme 2 g, diphenyl ether 3 g, CO_2 flow rate 200 mL min^{-1} , 333–483 K, 4 h. (e) CeO_2 0.10 g, 1,6-hexanediol 2.0 g (17 mmol), triglyme 2 g, diphenyl ether 3 g, CO_2 flow rate 0–350 mL min^{-1} , 483 K, 4 h.



points including *N*-methyl-2-pyrrolidone (NMP), tetraethylene glycol dimethyl ether (tetraglyme), tripropylene glycol dimethyl ether (isomer mixture, triPrglyme), diethylene glycol dibutyl ether (diglyBu), diphenylmethane, phenylcyclohexane, and diphenyl ether were applied to the reaction. The solvents with low solubility in water ($\leq 2 \text{ g L}^{-1}\text{-H}_2\text{O}$) including diglyBu, diphenylmethane, phenylcyclohexane, and diphenyl ether, provided higher conversion (4.7–5.2%) to the carbonates than triglyme (Fig. S5†). However, the solidification of 1,6-hexanediol occurred in the condenser due to their poor ability to dissolve 1,6-hexanediol (Table S5†), resulting in a lower diol balance (90–97%) and a difficulty in the prolonged reaction similar to the case of the neat conditions. On the other hand, the reactions with triglyme or tetraglyme that are miscible with water provided a higher diol balance (>99%) and adequate conversion (3.8%).

We estimated the ability of the solvents to retain water under the same reaction conditions by addition of water (0.10 g) in NMP, triglyme, triPrglyme, diglyBu, and diphenyl ether solvents, and the retained water amount in the solvent is called water affinity determined experimentally (Fig. 3b, *x*-axis, the detailed method is described in the ESI†). The solvents with lower solubility in water (diphenyl ether, $< 1 \text{ g L}^{-1}\text{-H}_2\text{O}$; diglyBu, $2 \text{ g L}^{-1}\text{-H}_2\text{O}$; triPrglyme, $280 \text{ g L}^{-1}\text{-H}_2\text{O}$) exhibited lower water affinity, and NMP, which is miscible with water and a highly polar aprotic solvent, showed higher water affinity. The conversion of the reaction of 1,6-hexanediol and CO_2 at 1 h was plotted as a function of the water affinity (Fig. 3b), showing a good relationship between the water affinity and conversion; the conversion decreased with higher water affinity. These results indicate that solvents with lower water affinity can promote the removal of water from the reaction media.

To achieve both high conversion and good diol balance, we studied a dual-solvent reaction system with a 2nd solvent in combination with triglyme (1st solvent) (Fig. 3c). The addition of NMP, which has higher water affinity, gave much lower conversion (1.1%) than that in the case of using 2 g of triglyme alone (3.8%), and the increase of the triglyme amount or combination with tetraglyme as a 2nd solvent also showed lower conversions (3.0%). The addition of solvents with lower water affinity such as triPrglyme, diglyBu, diphenylmethane, phenylcyclohexane, and diphenyl ether as a 2nd solvent gave higher conversion (4.1–4.7%) than that with triglyme alone (3.8%). Since diphenyl ether as a 2nd solvent provided higher conversion (4.7%) than the other solvents, diphenyl ether was selected as a 2nd solvent in combination with triglyme in an optimized ratio (2 g of triglyme and 3 g of diphenyl ether, Fig. S7 and S8†) and used in the subsequent experiments.

The effect of reaction temperature was investigated with an adequate amount of CeO_2 (0.10 g) in the range between 333 and 483 K, which is below the boiling point of the 1st solvent, triglyme (489 K) (Fig. 3d). The conversion increased with an increase in the reaction temperature from 333 K to 483 K, and production of the polymer was observed when the conversion exceeded 3% at temperatures above 373 K. The results suggest that a higher reaction temperature facilitates the removal of

water from the reaction media, which shifts the equilibrium to the product side to result in higher conversion.

The effect of the CO_2 flow rate was investigated in the presence of an adequate CeO_2 amount (0.10 g) (Fig. 3e). The conversion increased almost linearly with the increase of the CO_2 flow rate from 0 to 200 mL min^{-1} and became constant at 17% when the flow rate was above 200 mL min^{-1} . From the results, a CO_2 flow rate of 200 mL min^{-1} was selected for the subsequent synthesis of polycarbonate diol.

The effect of the mixed gas flow of CO_2 and N_2 was studied in the presence of an adequate amount of CeO_2 (0.10 g) (Fig. 4, left side, the detailed results are shown in Table S6†). The flow rate of CO_2 was fixed to 70 mL min^{-1} and the total flow rate was changed from 70 to 250 mL min^{-1} by N_2 flow. The conversions were not changed at any flow rates (70–250 mL min^{-1}). The behaviour is different from that with pure CO_2 flow (Fig. 4, right side, the detailed results are shown in Table S7†), where the higher CO_2 flow rate provided higher conversion in the range of 70–200 mL min^{-1} . These results indicate that the gas flow rate does not contribute to the removal of water, which can be explained by the low water concentration in the gas flow (0.38 g m^{-3}). A possible interpretation of the results is that a higher CO_2 flow rate increased the concentration of CO_2 in the reaction media, helping the equilibrium shift to the product side and afford higher conversion.

Fig. 5 shows the effect of the 1,6-hexanediol concentration on the reaction at 483 K. The CeO_2 amount was decreased to 0.03 g, where the rate-determining step is the reaction over CeO_2 , not the removal of water to shift the equilibrium (Fig. 3a). The conversion increased with an increase in the 1,6-hexanediol concentration at lower concentrations from 0.9 to 2.4 M (Fig. 5), and the selectivity to the dimer slightly decreased as it was polymerized into the polymer. At higher concentrations from 2.4 to 4.9 M, the conversion and selectivities were almost the same, suggesting that the adsorption of

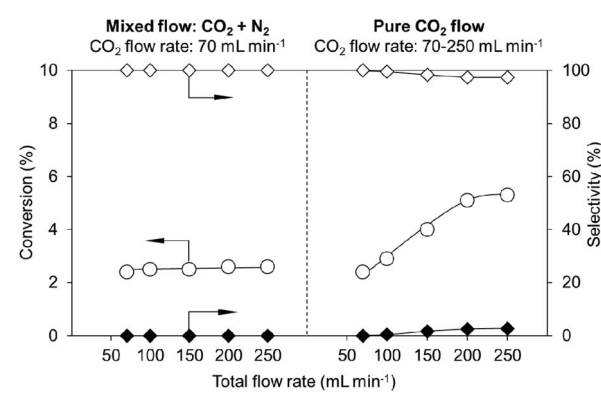


Fig. 4 Effect of mixed gas flow of CO_2 and N_2 in the reaction of flow CO_2 and 1,6-hexanediol with a CeO_2 catalyst. Reaction conditions: CeO_2 0.10 g, 1,6-hexanediol 2.0 g (17 mmol), triglyme 2 g, diphenyl ether 3 g, CO_2 flow rate 70 mL min^{-1} [compensated with N_2 (0–180 mL min^{-1}), left graph]; CO_2 flow rate 70–250 mL min^{-1} (right graph), 483 K, 1 h. O_2 , Conversion; \diamond , dimer selectivity; and \blacklozenge , polymer selectivity.



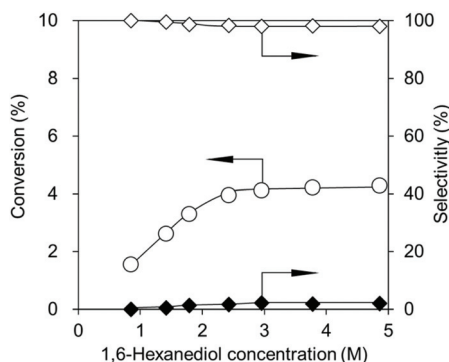


Fig. 5 Effect of the 1,6-hexanediol concentration in the reaction of flow CO_2 and 1,6-hexanediol with a CeO_2 catalyst. Reaction conditions: CeO_2 0.03 g, 1,6-hexanediol 2.0 g (17 mmol), solvent volume 1.5–18 mL (triglyme : diphenyl ether = 2 : 3 volume ratio), CO_2 flow rate 200 mL min^{-1} , 483 K, 1 h. \circ , Conversion; \diamond , dimer selectivity; and \blacklozenge , polymer selectivity.

1,6-hexanediol was saturated over CeO_2 . The standard reaction conditions were set at a concentration of 2.4 M, which was in this range.

Time-course of the reaction of 1,6-hexanediol and CO_2 over CeO_2 in the CO_2 flow semi-batch reactor and analyses of the produced polymer

Fig. 6a exhibits the time-course of the reaction of flow CO_2 and 1,6-hexanediol at 483 K with a CeO_2 catalyst and a mixture solvent of triglyme and diphenyl ether. The reaction proceeded smoothly to reach 95% conversion at 96 h. The selectivity to the dimer was high at a low conversion level and decreased with a longer reaction time, and conversely, the selectivity to the polymer kept increasing and reached 97% at 96 h. No non-polymeric by-product was observed during the reaction. The water content in the reaction media drastically decreased from 900 ppm to <4 ppm (below detection limit) during the heating-up to the reaction temperature of 483 K within several minutes and was unmeasurable at a longer reaction time. The conver-

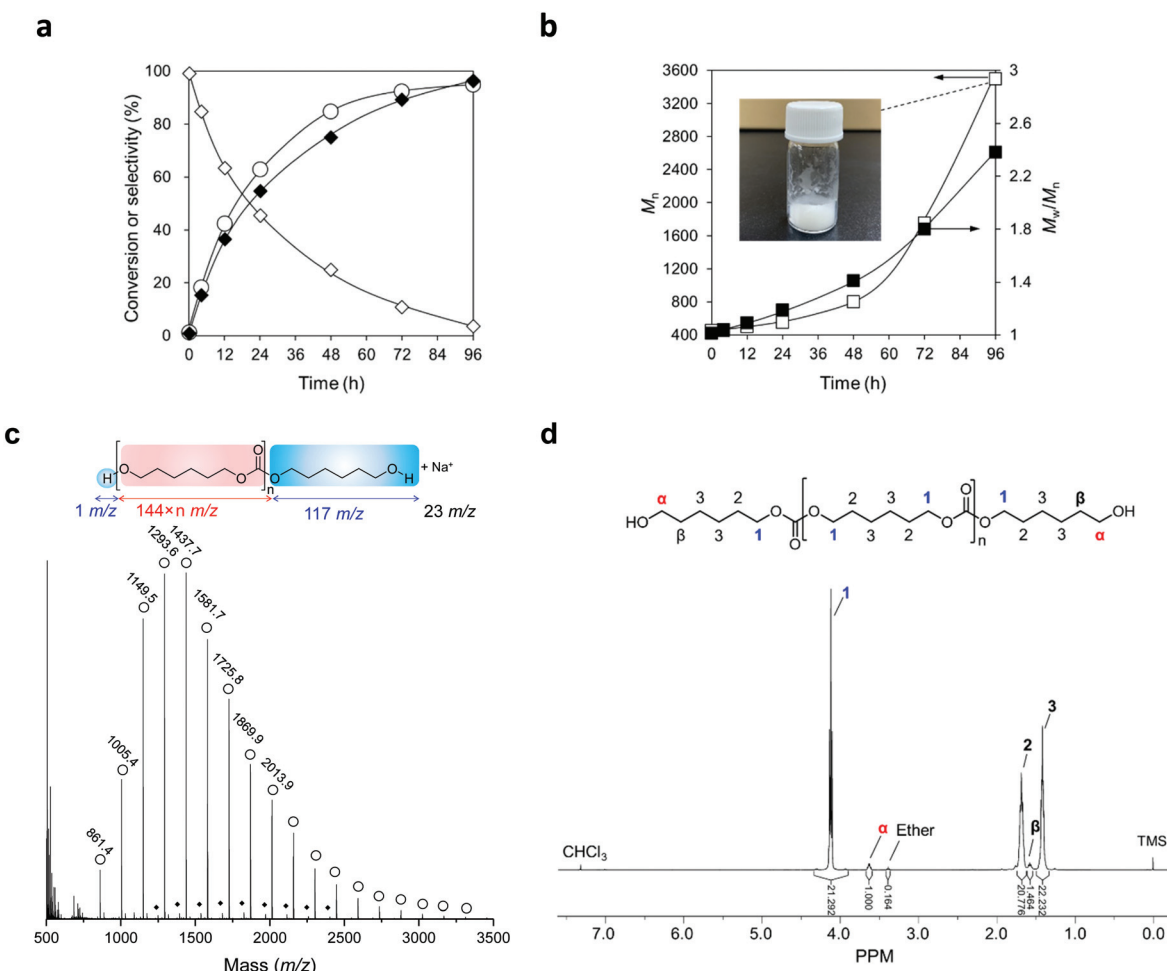


Fig. 6 Synthesis and characterization of polycarbonate diol from CO_2 and 1,6-hexanediol over CeO_2 in a CO_2 -flow reaction system: (a) Time-course and (b) molecular weight (M_n) and dispersity (M_w/M_n) profile. (c) MALDI-TOF/MS analysis. (d) ^1H -NMR analysis with CDCl_3 solvent. Marks in (a): \circ , Conversion; \diamond , dimer selectivity; and \blacklozenge , polymer selectivity; marks in (b) \square , M_n ; \blacksquare , M_w/M_n . Reaction conditions of (a) and (b): CeO_2 0.10 g, 1,6-hexanediol 2.0 g (17 mmol), triglyme 2 g, diphenyl ether 3 g, CO_2 flow rate 200 mL min^{-1} , 483 K, 0–96 h.

sion of CO_2 was also calculated using the data of the 4 h reaction, in which the dimer and the trimer were the only products. 2000 mmol of CO_2 were introduced into the reactor in 4 hours and the formation amount of the carbonates was 2 mmol, meaning that the conversion of CO_2 was 0.1%.

The average molecular weight (M_n) and dispersity (M_w/M_n) of the produced products were analysed by size-exclusion chromatography (SEC) (Fig. 6b). Both the M_n and M_w/M_n of the products kept increasing during the reaction, and polymer with an M_n of 3500 (in the case of polycarbonate diols, 24 repeating units) was obtained at 96 h. The increase of M_n became faster when higher conversion was achieved with a longer reaction time, which is a characteristic of step-growth polymerization.

The polymer produced at 96 h was isolated by precipitation (the detailed method is described in the ESI[†]), and the isolated polymer was a pure white wax-like solid (Fig. 6b). The isolated polymer was analysed by MALDI-TOF mass (Fig. 6c) and $^1\text{H-NMR}$ (Fig. 6d) spectroscopy (the detailed method is described in the ESI[†]). A series of strong signals with a mass increase of 144 was observed in MALDI-TOF mass spectrum and they were assigned to poly(hexamethylene carbonate) diol (Fig. 6c). The other series of minor signals with a lower mass number of 44 than the strong signals was identified as poly(hexamethylene carbonate) diol with one ether linkage. The ^1H NMR chart of the obtained polymer (Fig. 6d) showed the characteristic signals at 3.6 ppm (marked as “ α ” in the chart) and 4.0–4.2 ppm (marked as “1”), which can be assigned to the protons of the methylene group adjacent to the OH group and carbonate group, respectively. The average molecular weight of the isolated polycarbonate diol is estimated to be 3200 g mol⁻¹ by calculating the ratio of the proton numbers on the two positions (“ α ” and “1”). The value was similar to that determined by SEC (3500 g mol⁻¹ based on polystyrene standards). A triplet signal at 3.4 ppm is assigned to the protons of the methylene group adjacent to the ether bond, which is in agreement with the result of MALDI-TOF mass spectra, and the ratio of the ether linkage to the carbonate linkage is 0.8%. There were no signals at 4.9 and 5.8 ppm, where the vinylic proton appears (an enlarged chart is shown in Fig. S9[†]).

The proposed reaction mechanism of the polycarbonate diols from CO_2 and 1,6-hexanediol over CeO_2 is shown in Fig. 7 based on the previous reports on the synthesis of dimethyl carbonate from CO_2 and methanol over CeO_2 , where the reaction mechanism was proposed by the kinetic studies and analyses such as DRIFTS and isotopic labelling studies.^{64,79,93} The present reaction proceeded *via* the formation of dialkyl carbonate (dimer) from CO_2 and 1,6-hexanediol over CeO_2 (Fig. 6a), and hence the reaction mechanism of the present catalyst system would be similar to the previous one: (i) The dissociative adsorption of 1,6-hexanediol on the CeO_2 surface gives the alkoxide adspecies. (ii) The insertion of CO_2 into the alkoxide adspecies provides Ce-hydroxyhexyl carbonate adspecies. (iii) The nucleophilic attack of the oxygen anion in the alkoxide adspecies to the carbonate group in the Ce-hydroxyhexyl carbonate adspecies affords the corres-

Formation of the dimer:

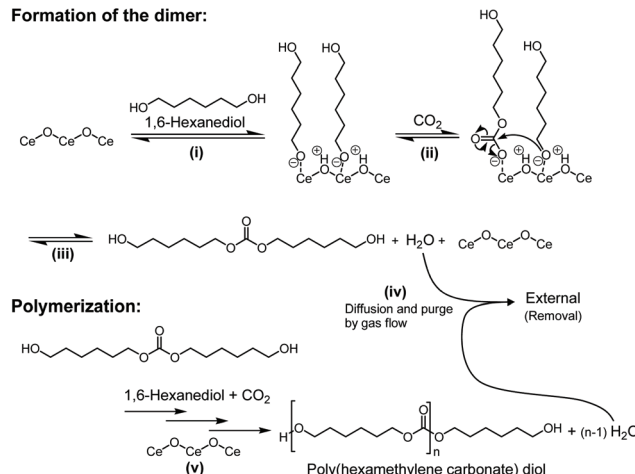


Fig. 7 Proposed reaction mechanism of the copolymerization of flow CO_2 and 1,6-hexanediol over a CeO_2 catalyst.

ponding linear carbonate (dimer). (iv) Diffusion and purge of the coproduced water from the reaction media to the gas phase by the gas flow. (v) Further reaction of the produced dimer with CO_2 and 1,6-hexanediol or the produced copolymer results in a step-growth polymerization with the production of poly(hexamethylene carbonate) diol. The water removal step in (iv) played a vital role in the reaction progress, which shifts the equilibrium and enables the dimer yield high enough to start the polymerization. Without this step, no products will be achieved under atmospheric pressure as shown in Table S3.[†] The high activity of CeO_2 for the reaction is due to the acid-base bifunctionality: CeO_2 has both weak acidic sites and medium basic sites, which can be used for the activation of CO_2 and alcohols.^{31,64,90} Side reactions catalysed by strong acid catalysts, which afford by-products such as ethers and alkenes, are also suppressed because of the weak acidity of CeO_2 .

The high durability of CeO_2 was confirmed by the reusability test (Fig. 8). 0.8 gram of the CeO_2 catalyst was

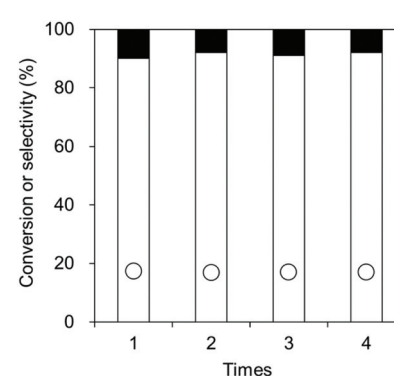
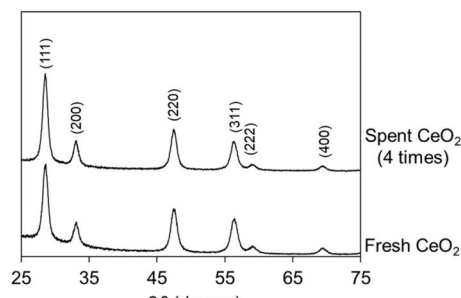


Fig. 8 Reusability test of the CeO_2 catalyst in the reaction of flow CO_2 and 1,6-hexanediol. ○: Conversion, white bar: dimer selectivity, and black bar: polymer selectivity. Reaction conditions: CeO_2 0.08 g, 1,6-hexanediol 2.0 g (17 mmol), triglyme 2.0 g, diphenyl ether 3.0 g, CO_2 flow rate 200 mL min⁻¹, 483 K, 4 h.





	BET surface area (m² g⁻¹)	Crystallite size (nm)
Spent CeO ₂ (4 times)	82	9.2
Fresh CeO ₂	84	9.1

Fig. 9 XRD patterns and BET surface area before and after the reuse test. The reaction results are shown in Fig. 8. The crystallite size of CeO₂ was estimated using the Scherrer equation [crystalline plane (111) was used for the estimation].

used, and a CeO₂ amount below 0.8 g would lead to a decrease in the conversion. The CeO₂ was used 4 times, providing similar conversions and selectivities. No distinct difference in the XRD patterns, crystallite size, and specific

surface area was observed between fresh CeO₂ catalyst and the spent CeO₂ catalyst which has been used 4 times (Fig. 9).

Substrate scope of the CO₂ flow reaction system with a CeO₂ catalyst

The scope of the reaction system was investigated with various alcohols (Table 1). C4–C10 α,ω -diols (entries 1–4) including *trans*-1,4-cyclohexanediethanol, an α,ω -diol with a rigid structure, provided the target dimer and polycarbonate diols in high selectivity (>99%). Moreover, 1-decanol (entry 6), a primary alcohol, also reacted to give the corresponding linear carbonate in high selectivity. In the case of 1,2-propanediol (entry 5) which has primary and secondary OH groups, the propylene carbonate, a cyclic organic carbonate, was obtained without the production of linear carbonates.

Conclusions

We demonstrated the direct transformation of atmospheric pressure flowing CO₂ with 1,6-hexanediol into the corresponding polycarbonate diol without any dehydration agents, achieving high yield and selectivity to the target polycarbonate

Table 1 Scope of alcohols in the synthesis of organic carbonates using flow CO₂ and alcohols

Entry	Alcohol	B.P. ^a (K)	T (K)	Conv. (%)	Selectivity (%)		
1	<chem>HOCCCCCO</chem>	523	483	85	 25	Polymer ^b 75	Others <1
2	<chem>HOCCCCCCCO</chem>	578	473	58	 52	Polymer ^b 48	Others <1
3	<chem>HOCCCCCO</chem>	508	453	30	 73	Polymer ^b 27	Others <1
4	<chem>HOCC1CCCCC1CO</chem>	558	473	55	 71	Polymer ^b 29	Others <1
5	<chem>HOCCCO</chem>	458	393	13	 >99	Polymer ^b <1	Others <1
6	<chem>CCCCCO</chem>	503	483	53	 >99	Others <1	

Reaction conditions: CeO₂ 0.10 g, alcohol 17 mmol, triglyme 2 g, diphenyl ether 3 g, CO₂ flow rate 200 mL min⁻¹, 393–483 K, 48 h. ^a Boiling point of the alcohols. ^b Polymers are defined as trimers and further polymerized into polycarbonate diols.

diol. CeO_2 worked as the most effective and reusable heterogeneous catalyst and the CO_2 flow system enabled the removal of water from the reaction media to overcome the reaction equilibrium. The wide applicability of the reaction system to other alcohols was confirmed and the corresponding organic (poly)carbonates were obtained in high selectivity (>99%). The developed catalyst system is expected to substitute for hazardous processes such as the phosgene process for the synthesis of polycarbonate diols and also contribute to the synthesis of other CO_2 -based organic carbonates with large molecular weights. Although the reaction conditions are comparatively severe at present, the catalyst system has high potential for the green process by the rationalization of the catalytic process.

Experimental

Materials

CeO_2 was prepared by calcining commercial CeO_2 (Daiichi Kigenso Kagaku Kogyo, purity of CeO_2 = 99.97%) in air at 873 K for 3 h, and the specific surface area (BET method) of the calcined CeO_2 is $84 \text{ m}^2 \text{ g}^{-1}$. Other commercial metal oxides including ZrO_2 (Daiichi Kigenso Kagaku Kogyo), SiO_2 (Fuji Silysia Chemical), $\gamma\text{-Al}_2\text{O}_3$ (Sumitomo Chemical), MgO (Ube Industries), and TiO_2 (Nippon Aerosil) were also calcined under the same conditions before use. La_2O_3 , Dy_2O_3 , Gd_2O_3 , Eu_2O_3 , Sm_2O_3 , Y_2O_3 , Pr_6O_{11} , and ZnO purchased from Kanto Chemical, and $\text{SiO}_2\text{-Al}_2\text{O}_3$ (product code: JRC-SAL-3) received from the Catalysis Society of Japan were used without any treatment. All the reagents and gases used in the experiments were used without further purification, which are as follows: 1,6-hexanediol (>97.0%, TCI (Tokyo Chemical Industry)), 1,10-decanediol (>97.0%, TCI), 1,4-butanediol (>98.0%, FUJIFILM Wako Pure Chemical), *trans*-1,4-cyclohexanediethanol (>98.0%, TCI), 1,2-propanediol (>99.0%, TCI), 1-decanol (>98.0%, TCI), diphenyl ether (>99.0%, TCI), triethylene glycol dimethyl ether (>99.0%, stabilized with BHT, TCI), and diethylene glycol dimethyl ether (>99.0%, TCI), 1-methyl-2-pyrrolidone (>99.0%, TCI), tetraethylene glycol dimethyl ether (>98.0%, TCI), dipropylene glycol dimethyl ether (mixture of isomers) (>94.0%, TCI), diethylene glycol dibutyl ether (>98.0%, TCI), diphenylmethane (>99.0%, TCI), phenylcyclohexane (>97.0%, TCI), CO_2 (G1 grade, purity $\geq 99.995 \text{ vol\%}$, $\text{H}_2\text{O} \leq 2.6 \text{ ppm}$, Taiyo Nippon Sanso), and N_2 (G1 grade, purity $\geq 99.9995 \text{ vol\%}$, $\text{H}_2\text{O} \leq 0.5 \text{ ppm}$).

Methods

General procedure for the reaction of 1,6-hexanediol and CO_2 in a CO_2 flow semi-batch reactor. The reaction was carried out in a set of glass apparatus including a 50 mL 3-neck pear-shaped flask at the bottom, a Graham's condenser (under ambient temperature) in the middle, and a glass trap filled with ethanol on the top (Fig. S2†). A catalyst and reagents were put into the flask, and then a PTFE tube for CO_2 introduction was inserted into the bottom of the flask. The glass apparatus

was finally set up, and the flask part was put into an oil bath for heating. When the reaction was done, the flask was transferred to an ice-water bath for cooling down. The ethanol in the glass trap was firstly collected with 1 g of diglyme (internal standard) added in for GC analysis. After the flask was cooled down to room temperature, 40 g of THF and 1 g of diglyme as an internal standard was injected in, and the mixture was collected for further analysis.

Procedure of the reaction carried out in an autoclave reactor. CeO_2 , 1,6-hexanediol, and a PTFE-coated magnetic spinner were put into a stainless-steel autoclave reactor with an inner volume of 190 mL. The autoclave was purged with 1 MPa CO_2 three times, and then pressurized to 5 MPa CO_2 [at room temperature, about 22 g (0.5 mol)]. The autoclave was then heated at 483 K (the heating-up took about 1 hour), and the pressure in the reactor increased to 7.5 MPa. The reaction was carried out for a designated reaction time, and then cooled in an ice water bath. The reaction mixture was collected in the same way noted in the general procedure.

Author contributions

Yu Gu: Investigation, methodology, formal analysis, and writing – original draft. Masazumi Tamura: Conceptualization, funding acquisition, formal analysis, and writing – original draft. Yoshinao Nakagawa: Writing – review & editing. Kenji Nakao: Formal analysis. Kimihito Suzuki: Formal analysis. Keiichi Tomishige: Formal analysis, supervision, and writing – review & editing.

Conflicts of interest

There are no conflicts to declare.

Acknowledgements

This paper is based on the results obtained from a “NEDO Feasibility Study Program” commissioned by the New Energy and Industrial Technology Development Organization (NEDO).

References

- 1 *Carbon Dioxide as Chemical Feedstock*, ed. M. Aresta, Wiley-VCH, Weinheim, Germany, 2010.
- 2 Q. Liu, L. Wu, R. Jackstell and M. Beller, *Nat. Commun.*, 2015, **6**, 5933.
- 3 M. Aresta, A. Dibenedetto and A. Angelini, *Chem. Rev.*, 2014, **114**, 1709–1742.
- 4 D. U. Nielsen, X.-M. Hu, K. Daasbjerg and T. Skrydstrup, *Nat. Catal.*, 2018, **1**, 244–254.
- 5 M. Aresta and A. Dibenedetto, *Front. Energy Res.*, 2020, **8**, 159.

6 C. S. Diercks, Y. Liu, K. E. Cordova and O. M. Yaghi, *Nat. Mater.*, 2018, **17**, 301–307.

7 Y. Y. Birdja, E. Pérez-Gallent, M. C. Figueiredo, A. J. Göttle, F. Calle-Vallejo and M. T. M. Koper, *Nat. Energy*, 2019, **4**, 732–745.

8 W. Li, H. Wang, X. Jiang, J. Zhu, Z. Liu, X. Guo and C. Song, *RSC Adv.*, 2018, **8**, 7651–7669.

9 L. Guo, J. Sun, Q. Ge and N. Tsubaki, *J. Mater. Chem. A*, 2018, **6**, 23244–23262.

10 W.-H. Wang, Y. Himeda, J. T. Muckerman, G. F. Manbeck and E. Fujita, *Chem. Rev.*, 2015, **115**, 12936–12973.

11 X. Jiang, X. Nie, X. Guo, C. Song and J. G. Chen, *Chem. Rev.*, 2020, **120**, 7984–8034.

12 J. R. Cabrero-Antonino, R. Adam and M. Beller, *Angew. Chem., Int. Ed.*, 2019, **58**, 12820–12838.

13 A. Álvarez, A. Bansode, A. Urakawa, A. V. Bavykina, T. A. Wezendonk, M. Makkee, J. Gascon and F. Kapteijn, *Chem. Rev.*, 2017, **117**, 9804–9838.

14 H. Yang, C. Zhang, P. Gao, H. Wang, X. Li, L. Zhong, W. Wei and Y. Sun, *Catal. Sci. Technol.*, 2017, **7**, 4580–4598.

15 X. Wang, H. Wang and Y. Sun, *Chem*, 2017, **3**, 211–228.

16 C. Chen, J. F. Khosrowabadi Kotyk and S. W. Sheehan, *Chem*, 2018, **4**, 2571–2586.

17 A. Modak, P. Bhanja, S. Dutta, B. Chowdhury and A. Bhaumik, *Green Chem.*, 2020, **22**, 4002–4033.

18 M. Cokoja, C. Bruckmeier, B. Rieger, W. A. Herrmann and F. E. Kühn, *Angew. Chem., Int. Ed.*, 2011, **50**, 8510–8537.

19 B. Yu and L.-N. He, *ChemSusChem*, 2015, **8**, 52–62.

20 Z. Chen, S. Du, J. Zhang and X.-F. Wu, *Green Chem.*, 2020, **22**, 8169–8182.

21 A. J. Kamphuis, F. Picchionia and P. P. Pescarmona, *Green Chem.*, 2019, **21**, 406–448.

22 D. J. Daresbourg, *Chem. Rev.*, 2007, **107**, 2388–2410.

23 X.-B. Lu and D. J. Daresbourg, *Chem. Soc. Rev.*, 2012, **41**, 1462–1484.

24 G. Fiorani, W. S. Guo and A. W. Kleij, *Green Chem.*, 2015, **17**, 1375–1389.

25 B. Grignard, S. Gennen, C. Jérôme, A. W. Kleij and C. Detrembleur, *Chem. Soc. Rev.*, 2019, **48**, 4466–4514.

26 C. Martín, G. Fiorani and A. W. Kleij, *ACS Catal.*, 2015, **5**, 1353–1370.

27 H. Sugimoto and S. Inoue, *J. Polym. Sci., Part A: Polym. Chem.*, 2004, **42**, 5561–5573.

28 K. Tomishige, Y. Gu, T. Chang, M. Tamura and Y. Nakagawa, *Mater. Today Sustainability*, 2020, **9**, 100035.

29 K. Tomishige, Y. Nakagawa and M. Tamura, *Chem. Rec.*, 2019, **19**, 1354–1379.

30 M. Tamura, M. Honda, Y. Nakagawa and K. Tomishige, *J. Chem. Technol. Biotechnol.*, 2014, **89**, 19–33.

31 K. Tomishige, Y. Gu, Y. Nakagawa and M. Tamura, *Front. Energy Res.*, 2020, **8**, 117.

32 Y. Gu, A. Miura, M. Tamura, Y. Nakagawa and K. Tomishige, *ACS Sustainable Chem. Eng.*, 2019, **7**, 16795–16802.

33 M. Tamura, A. Miura, M. Honda, Y. Gu, Y. Nakagawa and K. Tomishige, *ChemCatChem*, 2018, **10**, 4821–4825.

34 H.-Y. Yuan, J.-C. Choi, S. Onozawa, N. Fukaya, S. J. Choi, H. Yasuda and T. Sakakura, *J. CO₂ Util.*, 2016, **16**, 282–286.

35 Q. Zhang, H.-Y. Yuan, N. Fukaya, H. Yasuda and J.-C. Choi, *ChemSusChem*, 2017, **10**, 1501–1508.

36 J.-C. Choi, H.-Y. Yuan, N. Fukaya, S. Onozawa, Q. Zhang, S. J. Choi and H. Yasuda, *Chem. – Asian J.*, 2017, **12**, 1297–1300.

37 Q. Zhang, H.-Y. Yuan, N. Fukaya, H. Yasuda and J.-C. Choi, *Green Chem.*, 2017, **19**, 5614–5624.

38 Q. Zhang, H.-Y. Yuan, N. Fukaya and J.-C. Choi, *ACS Sustainable Chem. Eng.*, 2018, **6**, 6675–6681.

39 C. Claver, M. B. Yeamin, M. Reguero and A. M. Masdeu-Bultó, *Green Chem.*, 2020, **22**, 7665–7706.

40 G. A. Bhat, M. Luo and D. J. Daresbourg, *Green Chem.*, 2020, **22**, 7707–7724.

41 W. S. Putro, A. Ikeda, S. Shigeyasu, S. Hamura, S. Matsumoto, V. Y. Lee, J.-C. Choi and N. Fukaya, *ChemSusChem*, 2021, **14**, 842–846.

42 L. Guo, K. J. Lamb and M. North, *Green Chem.*, 2021, **23**, 77–118.

43 H. Chen, P. Chauhanb and N. Yan, *Green Chem.*, 2020, **22**, 6874–6888.

44 M. Tamura, K. Noro, M. Honda, Y. Nakagawa and K. Tomishige, *Green Chem.*, 2013, **15**, 1567–1577.

45 M. Tamura, K. Ito, Y. Nakagawa and K. Tomishige, *J. Catal.*, 2016, **343**, 75–85.

46 M. Tamura, M. Honda, K. Noro, Y. Nakagawa and K. Tomishige, *J. Catal.*, 2013, **305**, 191–203.

47 M. Honda, S. Sonehara, H. Yasuda, Y. Nakagawa and K. Tomishige, *Green Chem.*, 2011, **13**, 3406–3413.

48 H. Ohno, M. Ikhlayel, M. Tamura, K. Nakao, K. Suzuki, K. Morita, Y. Kato, K. Tomishige and Y. Fukushima, *Green Chem.*, 2021, **23**, 457–469.

49 E. Leino, P. Mäki-Arvela, V. Eta, D. Yu. Murzin, T. Salmi and J.-P. Mikkola, *Appl. Catal., A*, 2010, **383**, 1–13.

50 C.-F. Li and S.-H. Zhong, *Catal. Today*, 2003, **82**, 83–90.

51 A. Dibenedetto, M. Aresta, A. Angelini, J. Ethiraj and M. Aresta, *Chem. – Eur. J.*, 2012, **18**, 10324–10334.

52 P. Unnikrishnan, P. Varhadi and D. Srinivas, *RSC Adv.*, 2013, **3**, 23993–23996.

53 J. C. Choi, L. N. He, H. Yasuda and T. Sakakura, *Green Chem.*, 2002, **4**, 230–234.

54 K. Iwakabe, M. Nakaiwa, T. Sakakura, J.-C. Choi, H. Yasuda, T. Takahashi and Y. Ooshima, *J. Chem. Eng. Jpn.*, 2005, **38**, 1020–1024.

55 D. C. Stoian, E. Taboada, J. Llorca, E. Molins, F. Medina and A. M. Segarra, *Chem. Commun.*, 2013, **49**, 5489–5491.

56 M. Honda, M. Tamura, Y. Nakagawa and K. Tomishige, *Catal. Sci. Technol.*, 2014, **4**, 2830–2845.

57 A. Bansode and A. Urakawa, *ACS Catal.*, 2014, **4**, 3877–3880.

58 Q. Zhang, H.-Y. Yuan, X.-T. Lin, N. Fukaya, T. Fujitani, K. Sato and J.-C. Choi, *Green Chem.*, 2020, **22**, 4231–4239.

59 M. Tamura, K. Ito, M. Honda, Y. Nakagawa, H. Sugimoto and K. Tomishige, *Sci. Rep.*, 2016, **6**, 24038.



60 Y. Gu, K. Matsuda, A. Nakayama, M. Tamura, Y. Nakagawa and K. Tomishige, *ACS Sustainable Chem. Eng.*, 2019, **7**, 6304–6315.

61 T. Chang, M. Tamura, Y. Nakagawa, N. Fukaya, J.-C. Choi, T. Mishima, S. Matsumoto, S. Hamura and K. Tomishige, *Green Chem.*, 2020, **22**, 7321–7327.

62 M. Honda, M. Tamura, Y. Nakagawa, S. Sonehara, K. Suzuki, K.-i. Fujimoto and K. Tomishige, *ChemSusChem*, 2013, **6**, 1341–1344.

63 M. Honda, M. Tamura, K. Nakao, K. Suzuki, Y. Nakagawa and K. Tomishige, *ACS Catal.*, 2014, **4**, 1893–1896.

64 M. Honda, M. Tamura, Y. Nakagawa, K. Nakao, K. Suzuki and K. Tomishige, *J. Catal.*, 2014, **318**, 95–107.

65 K. Tomishige and K. Kunimori, *Appl. Catal., A*, 2002, **237**, 103–109.

66 M. Honda, A. Suzuki, B. Noorjahan, K.-i. Fujimoto, K. Suzuki and K. Tomishige, *Chem. Commun.*, 2009, 4596–4598.

67 M. Honda, S. Kuno, B. Noorjahan, K.-i. Fujimoto, K. Suzuki, Y. Nakagawa and K. Tomishige, *Appl. Catal., A*, 2010, **384**, 165–170.

68 M. Honda, S. Kuno, S. Sonehara, K.-i. Fujimoto, K. Suzuki, Y. Nakagawa and K. Tomishige, *ChemCatChem*, 2011, **3**, 365–370.

69 T. Zhao, X. Hu, D. Wu, R. Li, G. Yang and Y. Wu, *ChemSusChem*, 2017, **10**, 2046–2052.

70 S. Kumar, P. Kumar and S. L. Jain, *J. Mater. Chem. A*, 2014, **2**, 18861–18866.

71 S. Verma, R. B. N. Baig, M. N. Nadagouda and R. S. Varma, *Sci. Rep.*, 2017, **7**, 655.

72 S. Kumar, M. B. Gawande, I. Medřík, M. Petr, O. Tomanec, V. Kupka, R. S. Varma and R. Zbořil, *Green Chem.*, 2020, **22**, 5619–5627.

73 A. Poungsombate, T. Imyen, P. Dittanet, B. Embley and P. Kongkachuchay, *J. Taiwan Inst. Chem. Eng.*, 2017, **80**, 16–24.

74 R. Nakano, S. Ito and K. Nozaki, *Nat. Chem.*, 2014, **6**, 325–331.

75 Y.-C. Xu, H. Zhou, X.-Y. Sun, W.-M. Ren and X.-B. Lu, *Macromolecules*, 2016, **49**, 5782–5787.

76 Y. Zhang, J. Xia, J. Song, J. Zhang, X. Ni and Z. Jian, *Macromolecules*, 2019, **52**, 2504–2512.

77 Z. Chen, N. Hadjichristidis, X. Feng and Y. Gnanou, *Polym. Chem.*, 2016, **7**, 4944–4952.

78 S. Oi, K. Nemoto, S. Matsuno and Y. Inoue, *Macromol. Rapid Commun.*, 1994, **15**, 133–137.

79 Z.-J. Gong, Y.-R. Li, H.-L. Wu, S. D. Lin and W.-Y. Yu, *Appl. Catal., B*, 2020, **265**, 118524.

80 Y.-C. Yu, T.-Y. Wang, L.-H. Chang, P.-J. Wu, B.-Y. Yu and W.-Y. Yu, *J. Taiwan Inst. Chem. Eng.*, 2020, **116**, 36–42.

81 J. Shang, S. Liu, X. Ma, L. Lu and Y. Deng, *Green Chem.*, 2012, **14**, 2899–2906.

82 Z. Ying, Y. Dong, J. Wang, Y. Yu, Y. Zhou, Y. Sun, C. Zhang, H. Cheng and F. Zhao, *Green Chem.*, 2016, **18**, 2528–2533.

83 S. Jiang, H.-Y. Cheng, R.-H. Shi, P.-X. Wu, W.-W. Lin, C. Zhang, M. Arai and F.-Y. Zhao, *ACS Appl. Mater. Interfaces*, 2019, **11**, 47413–47421.

84 R. Liu, X. Liu, K. Ouyang and Q. Yan, *ACS Macro Lett.*, 2019, **8**, 200–204.

85 Polycarbonate market size worth \$25.37 Billion by 2024, <https://www.grandviewresearch.com/press-release/global-polycarbonate-market>, (accessed June 2021).

86 S. Fukuoka, I. Fukawa, T. Adachi, H. Fujita, N. Sugiyama and T. Sawa, *Org. Process Res. Dev.*, 2019, **23**, 145–169.

87 S. Fukuoka, M. Kawamura, K. Komiya, M. Tojo, H. Hachiya, K. Hasegawa, M. Aminaka, H. Okamoto, I. Fukawa and S. Konno, *Green Chem.*, 2003, **5**, 497–507.

88 *Separation Process Principles*, ed. J. D. Seader and E. J. Henley, John Wiley & Sons Inc., Hoboken NJ, 2006, ch. 6, pp. 193–242.

89 Y.-L. Hwang, G. E. Keller II and J. D. Olson, *Ind. Eng. Chem. Res.*, 1992, **31**, 1753–1759.

90 K. Tomishige, T. Sakaihori, Y. Ikeda and K. Fujimoto, *Catal. Lett.*, 1999, **58**, 225–229.

91 S. Roy, G. Mpourmpakis, D.-Y. Hong, D. G. Vlachos, A. Bhan and R. J. Gorte, *ACS Catal.*, 2012, **2**, 1846–1853.

92 M. A. Ardagh, Z. Bo, S. L. Nauert and J. M. Notestein, *ACS Catal.*, 2016, **6**, 6156–6164.

93 Y. Yoshida, Y. Arai, S. Kado, K. Kunimori and K. Tomishige, *Catal. Today*, 2006, **115**, 95–101.

